Published in final edited form as:
Stem Cells. 2010 November ; 28(11): 2027–2040. doi:10.1002/stem.525.

Convergent Genesis of an Adult Neural Crest-Like Dermal Stem Cell from Distinct Developmental Origins

Hiroyuki Jinno[a,b], **Olena Morozova**[c], **Karen L. Jones**[a], **Jeffrey A. Biernaskie**[a,d], **Maryline Paris**[a], **Ryoichi Hosokawa**[e], **Michael A. Rudnicki**[f], **Yang Chai**[e], **Fabio Rossi**[g], **Marco A. Marra**[c], and **Freda D. Miller**[a,b,h]

[a] Developmental and Stem Cell Biology Program, The Hospital for Sick Children, Toronto, Canada

[b] Department of Physiology, University of Toronto, Toronto, Canada

[h] Department of Molecular Genetics, University of Toronto, Toronto, Canada

[c] Genome Sciences Center, British Columbia Cancer Agency, University of British Columbia, Vancouver, Canada

[g] The Biomedical Research Centre, University of British Columbia, Vancouver, Canada

[d] Department of Comparative Biology and Experimental Medicine, University of Calgary, Calgary, Canada

[e] Center for Craniofacial Molecular Biology, School of Dentistry, University of Southern California, Los Angeles, California, USA

[f] The Sprott Center for Stem Cell Research, University of Ottawa, Ottawa, Canada

Abstract

Skin-derived precursors (SKPs) are multipotent dermal stem cells that reside within a hair follicle niche and that share properties with embryonic neural crest precursors. Here, we have asked whether SKPs and their endogenous dermal precursors originate from the neural crest or whether, like the dermis itself, they originate from multiple developmental origins. To do this, we used two different mouse Cre lines that allow us to perform lineage tracing: *Wnt1-cre*, which targets cells deriving from the neural crest, and *Myf5-cre*, which targets cells of a somite origin. By crossing these Cre lines to reporter mice, we show that the endogenous follicle-associated dermal precursors in the face derive from the neural crest, and those in the dorsal trunk derive from the somites, as do the SKPs they generate. Despite these different developmental origins, SKPs from these two locations are functionally similar, even with regard to their ability to differentiate into Schwann cells, a cell type only thought to be generated from the neural crest. Analysis of global gene expression using microarrays confirmed that facial and dorsal SKPs exhibit a very high

Correspondence: Freda D. Miller, Ph.D., Hospital for Sick Children, MaRS Center, TMDT East Tower, 101 College St., #12-313, Toronto, Ontario, Canada M5G 1L7. Telephone: 416-813-7654 ext. 1434; Fax: 416-813-2212; fredam@sickkids.ca.

Disclosure of Potential Conflicts of Interest

The authors indicate no potential conflicts of interest.

Author contributions: H.J.: conception and design, collection of data, data analysis and interpretation, manuscript writing; O.M.: data analysis and interpretation, manuscript writing; K.L.J.: conception and design, collection of data; J.A.B.: conception and design, collection of data; M.P.: conception and design, collection of data; R.H.: provision of study material; M.A.R.: provision of study material, final approval of manuscript; Y. C.: provision of study material, final approval of manuscript; F. R.: provision of study material, final approval of manuscript; M.A.M.: data analysis and interpretation, final approval of manuscript; F.D.M.: conception and design, data analysis and interpretation, financial support, manuscript writing.

degree of similarity, and that they are also very similar to SKPs derived from ventral dermis, which has a lateral plate origin. However, these developmentally distinct SKPs also retain differential expression of a small number of genes that reflect their developmental origins. Thus, an adult neural crest-like dermal precursor can be generated from a non-neural crest origin, a finding with broad implications for the many neuroendocrine cells in the body.

Keywords

Dermis; Stem cells; Lineage tracing; Neural crest; Somites

Introduction

Over the past decade, it has become apparent that most adult tissues contain somatic tissue stem cells that serve, at least in part, to maintain those tissues. However, the genesis of these somatic tissue stem cells is still not very well understood. In this regard, we previously identified a population of dermal stem cells that originate during embryogenesis and persist into adulthood. These skin-derived precursor cells (SKPs) grow in suspension in response to fibroblast growth factor-2 (FGF2) and epidermal growth factor (EGF), and share properties with neural crest precursors, differentiating into mesenchymal derivatives such as adipocytes and skeletogenic cells [1, 2] and peripheral neural crest cell types such as Schwann cells [1, 3–6]. Recently, we demonstrated that SKPs derive from a *Sox2*-positive dermal precursor that resides within the dermal papilla (DP) and dermal sheath (DS) of hair and whisker follicles [7]. These endogenous dermal precursors are transcriptionally similar to SKPs, and, like SKPs, they are able to induce hair follicle morphogenesis and generate differentiated dermal cell types [7]. Moreover, genetic perturbations that disrupt the maintenance of these dermal-derived precursors, such as deletion of the p53 family member, *TAp63*, lead to aberrant wound-healing and premature tissue aging [8]. Thus, like other adult tissues, the dermis contains a somatic stem cell that is generated during embryogenesis and that may well serve to maintain and even repair that tissue.

Although the existence of dermal stem cells would be predicted by the highly regenerative nature of adult skin, the finding that they display similarities to neural crest precursors is somewhat surprising. In this regard, facial dermis derives from the neural crest embryonically [9], and SKPs generated from facial skin are neural crest-derived [6], raising the possibility that their hair follicle niche somehow maintains these dermal precursors in a multipotent, embryonic state. However, the dermis of the dorsal trunk does not come from the neural crest but is instead generated from the somites, specifically from the dermomyotome. Despite this, SKPs from dorsal trunk generate cell types only thought to be made from the neural crest such as Schwann cells [9, 10]. One explanation for this finding is that neural crest precursors invade the dorsal dermis during embryogenesis, and that it is these precursors that associate with hair follicles and generate SKPs. Support for this idea comes from our previous work showing that a small subpopulation of cells within and/or adjacent to the DP of dorsal hair follicles express a reporter thought to be limited to neural crest-derived cells [6], and a recent study showing that melanocytes are, at least in part, generated from multipotent neural crest precursors that enter the skin via peripheral nerves [11]. Moreover, neural crest-like precursors are present and persist in a number of other adult tissues, including peripheral ganglia [12, 13], gut [14], heart [15], skin [1, 6, 16, 17], cornea [18], carotid body [19], and palate [20]. An alternative explanation is that neural crest-like precursors are somehow generated from a different developmental origin. Conceptual support for this idea comes from the fact that many tissues contain neuroendocrine cells of nonneural crest origin, suggesting the existence of a second developmental pathway that converges on to a neural crest-like phenotype. Precedent for

such a convergent development model comes from the dermis itself; cells from the neural crest, somites, and lateral plate generate the dermis in the face [21], dorsal trunk [22], and ventral trunk [23], respectively.

Here, we have tested these two possibilities, taking advantage of genetically defined lineage tracing approaches. Our data demonstrate that SKPs, and the endogenous dermal precursors from which they derive, originate from the neural crest in the face and the somites in the dorsal trunk, but that despite these different origins, they both generate precursors with a highly similar phenotype. These findings provide precedent for the idea that somatic tissue stem cells can derive from multiple developmental origins, and suggest that neural crest-like precursors can derive from non-neural crest origins.

Materials and Methods

Animals

Wnt1-cre mice [24] (Tg[Wnt1-cre]11Rth Tg[Wnt1-GAL4]11Rth/J) and *Z/EG* reporter mice [25] (B6.129[Cg]-Tg[CAG-Bgeo/green fluorescent protein (GFP)]21Lbe/J) were purchased from JaxMice (Jackson Laboratories, Bar Harbor, ME, http://jaxmice.jax.org) and were crossed to obtain *Wnt1-cre;Z/EG* double-transgenic mice. *Myf5-cre* mice [26] (B6;129S4-*Myf5*$^{tm3(cre)Sor}$/J) were mated with *R26YFP* reporter mice [27] (B6.129X1-*Gt(ROSA)26Sor*$^{tm1(EYFP)Cos}$/J) or *R26R* mice [28] (B6;129S-*Gt(ROSA)26Sor*/J) to obtain *Myf5-cre;R26YFP* or *Myf5-cre;R26R* double-transgenic mice, and were maintained as previously reported [29, 30]. *Sox2-EGFP* mice [31] were the kind gift of Dr. Larysa Pevny and were maintained as previously reported [7]. Wild-type mice (C57BL/6 and CD1) and rats (Sprague-Dawley) were purchased from Charles River Laboratory (Wilmington, MA, http://www.criver.com). All animal use was approved by the Animal Care Committee for the Hospital for Sick Children in accordance with the Canadian Council of Animal Care policies.

Tissue Culture

SKPs were cultured as described [6]. Briefly, dorsal back, ventral trunk, and facial whisker pad skin from neonatal (P0–P5) or adult mice (3 weeks and older) were dissected and cut into 2–3 mm^2 pieces. For the microarray experiments, tissue was dissected from adult Sprague-Dawley rats. Rats were chosen to provide a direct comparison with adult rat mesenchymal stromal cells (MSCs). Tissue was digested with 1 mg/ml collagenase (type XI; Sigma-Aldrich, St. Louis, MO, http://www.sigmaaldrich.com) for 20–45 minutes at 37°C, mechanically dissociated and filtered through a 40-μm cell strainer (BD Falcon). Dissociated cells were pelleted and plated in Dulbecco's modified Eagle's medium (DMEM)-F12 (3:1; Invitrogen, Carlsbad, CA, http://www.invitrogen.com), containing 1% penicillin/streptomycin (Cambrex, East Rutherford, NJ, http://www.cambrex.com), 2% B27 supplement (Invitrogen), 20 ng/ml EGF, and 40 ng/ml FGF2 (BD Bioscience, San Diego, CA, http://www.bdbiosciences.com), hereafter referred to as proliferation medium. Primary spheres generated after 7–21 days were passaged by collagenase digestion and resuspended as single cells at densities ranging from 1,000 to 25,000 cells/ml. Second passage spheres (or greater) were used for all assays, unless otherwise indicated. MSCs were isolated from the bone marrow of adult GFP-expressing (Japan SLC, Hamamatsu, Japan, http://jslc.co.jp) or control Sprague-Dawley rats as described [32]. MSCs were maintained by plating on uncoated culture dishes at a density of 50,000 cells/ml Mesencult human MSC medium containing 10% fetal bovine serum (both from STEMCELL Technologies, Vancouver, Canada, http://www.stemcell.com). For SKP self-renewal assays, primary SKPs were dissociated and plated at 2,500 cells/ml in proliferation medium containing 1.6% methylcellulose (Sigma), as previously described [6]. Sphere formation was scored after 8–

14 days. Schwann cell differentiations in mass cultures were performed as previously described [3, 4]. For single sphere differentiations [3], single rat SKP spheres, at passage 1 were plated onto eight-well slides (Nunc/Thermo Fisher Scientific, Roskilde, Denmark, http://www.nuncbrand.com) coated with poly-L-lysine (Sigma) and laminin (BD Biosciences). Spheres were plated in Schwann cell proliferation medium for 3 days and then changed into Schwann cell differentiation medium for the following 14 days. Schwann cell proliferation medium consisted of DMEM:F-12 (3:1) (Invitrogen), 10% fetal calf serum (FCS) (Stem Cell Technologies), 1% B27 (invitrogen), 1% N2 (Invitrogen), 40 ng/ml FGF2 (Peprotech, Rocky Hill, NJ, http://www.peprotech.com), and 20 ng/ml EGF (BD Bioscience) and Schwann cell differentiation medium consisted of DMEM:F-12 (3:1), 2% N2 (Invitrogen), 25 ng/ml neuregulin-1β (R&D Systems, Minneapolis, MN, http://www.rndsystems.com), and 5 μM forskolin (Sigma). Medium was changed every 2–3 days.

Cell Sorting and Analysis

Dorsal back or facial whisker pad skin from neonatal (P0–P5) *Wnt1-cre;Z/EG*, *Myf5-cre;R26YFP*, or *Sox2-EGFP* mice was enzymatically digested and dissociated to single cell suspensions as described earlier. Cells were suspended in phosphate buffered saline (PBS) containing 1% bovine serum albumin and sorted for enhanced green fluorescent protein (EGFP) or enhanced yellow fluorescent protein (EYFP) expression on either MoFlo (Dako, Glostrup, Denmark, http://www.dako.com) or FACsAria (Becton Dickinson) cell sorters. Viable cells were identified by propidium iodide exclusion. Fractionated cells were subsequently grown in proliferation medium at densities of 5,000–20,000 cells/ml. For Schwann cell assays, SKP spheres generated from sorted cells were passaged once, and then differentiated under Schwann cell conditions for 3 weeks as described earlier in preparation for coculture with axons of rat sympathetic neurons grown in compartmented cultures as previously described [33]. Briefly, sympathetic neurons dissected from the superior cervical ganglion (SCG) of P1 Sprague-Dawley rats were dissociated and plated on a collagen substrate at a density of 0.6 ganglia/dish in 35-mm dishes in compartmented cultures. Neurons were established for 5–7 days in UltraCULTURE (Lonza, Basel, Switzerland, http://www.lonza.com), 2 mM L-glutamine (Lonza), 1% penicillin/streptomycin (Lonza) with 20 ng/ml nerve growth factor (NGF; CEDARLANE, Burlington, Canada, http://www.cedarlanelabs.com), conditions that allow the growth of axons into side compartments. Cultures were then maintained in the presence of 10 ng/ml NGF in both center and side compartments. *Myf5-cre;R26YFP* SKPs differentiated in Schwann cell conditions were then plated into the side compartments (8,000 cells/side) in Schwann cell differentiation medium with the addition of 10 ng/ml NGF. The cells were maintained on the axons for 8 days with a medium change every 2–3 days.

Microarrays and Bioinformatics

RNA was prepared from twice-passaged adult rat dorsal, facial, and ventral SKPs and MSCs using Trizol (Invitrogen), as per the manufacturer's instructions, followed by the RNeasy Mini Kit (Qiagen, Venlo, Netherlands, http://www.qiagen.com). The RNA samples were analyzed on Affymetrix Gene-Chip Rat Gene 1.0 ST Arrays (Affymetrix, Santa Clara, CA, http://www.affymetrix.com). The data were background corrected and normalized using standard robust multichip average (RMA) procedure implemented in the Affymetrix Expression Console software. The preprocessed data were analyzed using the LIMMA Bioconductor package to identify genes that show significant evidence of differential expression between SKPs and MSCs. The F-statistic with Benjamini-Hochberg (BH) multiple testing correction implemented in the eBayes function was used to assess significance of differential gene expression. Those genes with BH-corrected p value < .01

were considered statistically significant as per Smyth [34]. Microarray data are deposited in the NIH GEO repository (accession number GSE23954).

Reverse Transcription Polymerase Chain Reaction

RNA was prepared from twice-passaged neonatal mouse dorsal and facial SKPs using Trizol (Invitrogen) and from sorted, uncultured mouse skin cells using Cells-to-cDNA II kit (Ambion/Applied Biosystems, Austin, TX, http://www.ambion.com) as per the manufacturer's instructions, followed by the RNeasy Mini Kit (Qiagen). For all analyses, controls were performed without reverse transcriptase. Polymerase chain reaction (PCR) reactions were performed as follows: 94°C, 2 minutes; 25–35 cycles of 94°C, 15 seconds; gene-specific annealing temperature for 30 seconds; and 72°C for 30 seconds. Primers used in this study were as follows: *Ap2a1*, 5′-TCCCTG TCCAAGTCCAACAGCAAT-3′ and 5′-AAATTCG GTTTCGCACACGTACCC-3′; *Eya1*, 5′-CTAACCAGCCCGCATAGCCG-3′ and 5′-TAGTTTGTGAGGAAGGGGTAGG-3′; *Foxd3*, 5′-TCTTACATCGCGCTCATCAC-3′ and 5′-TCTT GACGAAGCAGTCGTTG-3′; *Gapdh*, 5′-CGTAGACAAAAT GGTGAAGGTCGG-3′ and 5′-AAGCAGTTGGTGGTGCAG GATG-3′; *Hoxa5*, 5′-TAGTTCCGTGAGCGAACAATTC-3′ and 5′-GCTGAGATCCATGCCATTGTAG-3′; *Hoxc4*, 5′-AA CCCATAGTCTACCCTTGGATGA-3′ and 5′-CGGTTGTAA TGAAACTCTTTCTCTAATTC-3′; *Hoxc6*, 5′-ACGTCGCCC TCAATTCCA-3′ and 5′-CTGAGCTACGGCTGCTCCAT-3′; *Hoxc9*, 5′-TGTAGCGATTTTCCGTCCTGTAG-3′ and 5′-CC GTAAGGGTGATAGACCACAGA-3′; *Mab21l1*, 5′-CCCCAA CATGATCGCGGCCCAGGCC-3′ and 5′-CCTCCTTCAGGA CGTCGGAGACCAC-3′; *Mab21l2*, 5′-CCCCAACATGATC GCCGCTCAGGCC-3′ and 5′-GCGGGGCTCTTGCACCTCC ACTTCC-3′; *Msx1*, 5′-CGGGCGCCTCACTCTACAGT-3′ and 5′-TCCCGCTGCTCTGCTCAAA-3′; *p75NTR*, 5′-GTG TTCTCCTGCCAGGACAA-3′ and 5′-GCAGCTGTTCCACC TCTTGA-3′; *Pax3*, 5′-TGCCCTCAGTGAGTTCTATCAGC-3′ and 5′-GCTAAACCAGACCTGCACTCGGGC-3′; *Rhob*, 5′-AAGACGTGCCTGCTGATCGTG-3′ and 5′-CTTGCAGC AGTTGATGCAGCC-3′; *Slug*, 5′-CGTCGGCAGCTCCACTC CACTCTC-3′ and 5′-TCTTCAGGGCACCCAGGCTCACAT-3′; *Snail1*, 5′-CGGCGCCGTCGTCCTTCT-3′ and 5′-GGCCT GGCACTGGTATCTCTTCAC-3′; *Sox9*, 5′-CCGCCCATCA CCCGCTCGCAATAC-3′ and 5′-GCCCCTCCTCGCTGATA CTGGTG-3′; *Sox10*, 5′-CAAGGGGCCCGTGTGCTA-3′ and 5′-GCCCGTGCCATGCTAACTCT-3′; *Twist1*, 5′-CTTTCCG CCCACCCACTTCCTCTT-3′ and 5′-GTCCACGGGCCTGT CTCGCTTTCT-3′; and *Zic1*, 5′-GCGGCCGAAAGCCAACT-3′ and 5′-TGCCAAAAGCAATGGACAGC-3′.

Immunocytochemistry and Histology

Immunocytochemistry was performed as described [7], and immunofluorescence was analyzed using a Zeiss upright fluorescence microscope with Northern Eclipse acquisition software, a Zeiss LSM 5 Pascal confocal microscope (Carl Zeiss, Oberkochen, Germany, http://www.zeiss.com), or a spinning disk confocal microscope using Velocity acquisition software (Improvision/PerkinElmer, Coventry, England, http://www.improvision.com). Cell nuclei and tissue morphology were visualized using Hoechst 33,258 (Sigma), TO-PRO-3 (Invitrogen), or propidium iodide (Sigma). X-gal staining was performed as described [6], and cells or tissue sections were counterstained with nuclear fast red (Sigma). Primary antibodies used in this study were as follows: mouse anti-*β*-galactosidase (1:50; Developmental Studies Hybridoma Bank/University of Iowa, Iowa City, IA, http://dshb.biology.uiowa.edu), rabbit anti-Fibronectin (1:400; Sigma Aldrich), rabbit anti-glial fibrillary acidic protein (GFAP) (1:1,000; Dako), chicken anti-GFP (1:1,000; Millipore, Billerica, MA, http://www.millipore.com), rabbit anti-GFP (1:1,000; Millipore), rabbit anti-

GFP (1:5,000; Abcam, Cambridge, England, http://www.abcam.com), mouse anti-Ki67 (1:200; BD Pharmingen, San Diego, CA, http://www.bdbiosciences.com), rat anti-neural cell adhesion molecule (NCAM) (1:500; Millipore), mouse anti-Nestin (1:400; BD Pharmingen), chicken anti-P0 (1:250; Aves Labs, Tigard, OR, http://www.aveslab.com), rat anti-PDGFRα (1:500; eBioscience, San Diego, CA, http://www.ebioscience.com), rabbit anti-p75NTR (1:500; Promega), mouse anti-S100β (1:1,000; Sigma Aldrich), rabbit anti-tyrosinase-related protein 1 (TRP1) (1:500; Santa Cruz), rabbit anti-Tyrosinase (1:500; Santa Cruz), rabbit anti-Versican (1:500; kind gift from R. LeBaron, U.T.S.A.), and mouse anti-Vimentin (1:200; BD Pharmingen), anti-βIII-tubulin (1:500, Covance). Secondary antibodies used in this study were as follows: Alexa488-conjugated goat anti-mouse, anti-rabbit, or anti-chicken, Alexa555 goat anti-mouse, anti-rabbit or anti-chicken and Alexa647 goat anti-rabbit, anti-mouse or anti-rat (1:1,000; all from INVITROGEN).

Statistics

Statistics (with exception of the microarray analyses) were performed using two-tailed *t* tests or one-way analysis of variance (ANOVA) where appropriate, and represented as mean ± SEM. All experiments were performed at least in triplicate.

Results

Hair Follicle DP and DS Are Neural Crest-Derived in Facial but Not Dorsal Trunk Skin

We recently showed that SKPs derive from a *Sox2*-positive precursor associated with follicle DP and DS in both trunk and facial skin [7]. To ask if these endogenous dermal precursors were neural crest-derived, we performed lineage tracing using a *Wnt1-cre* mouse [24], which specifically targets Cre recombinase to neural crest derivatives in the periphery. We crossed this mouse to the *Z/EG* reporter mouse [25], where active Cre recombinase will knock in an EGFP reporter, thereby allowing us to trace neural crest progeny by monitoring EGFP expression. We then analyzed neonatal facial and dorsal trunk skin of these crossed mice, performing triple-label analysis for EGFP to trace neural crest cells, NCAM, a marker for the follicle DP and DS, and tyrosinase, a marker for melanoblasts/melanocytes that are present in the hair follicle. This analysis showed that, in facial skin, DP, and DS cells of almost all hair and whisker follicles were EGFP-positive (Fig. 1A, 1B), as were the majority of cells within the interfollicular dermis (data not shown), indicating that facial dermis derives from *Wnt1*-expressing neural crest cells, as previously reported [6, 13]. In contrast, in dorsal skin, NCAM-positive DS and DP cells of hair follicles were uniformly EGFP-negative (Fig. 1C), as were cells of the interfollicular dermis. However, EGFP was expressed in two neural crest cell types in dorsal skin, tyrosinase-positive melanocytes (Fig. 1C, 1D), and P0-positive myelinating and p75NTR-positive nonmyelinating Schwann cells (Fig. 1E). Quantification showed that at least 70%–80% of dorsal skin melanocytes and Schwann cells expressed EGFP, demonstrating that the reporter gene is highly penetrant. EGFP was also expressed in cells located near the bulge region, where they were closely associated with p75NTR-positive nerve fibers (data not shown), consistent with previous work documenting *Wnt1-cre;R26R*-positive cells in the bulge region [35]. Thus, follicle DP and DS cells are neural crest-derived in the face, whereas those of the dorsal trunk apparently have another developmental origin.

Facial, but Not Trunk, SKPs Are Neural Crest-Derived

We [6] and others [13] previously showed that SKPs from facial skin are neural crest-derived. To ask whether SKPs from dorsal trunk skin had a different developmental origin, as suggested by the in vivo lineage tracing, we cultured SKPs from dorsal versus facial skin of neonatal *Wnt1-cre;Z/EG* mice. To do this, skin cells were dissociated and cultured at low density under nonadherent conditions in the presence of EGF and FGF2; in these conditions,

SKPs will grow and proliferate as spheres. As previously documented, virtually all of the SKP spheres isolated from facial skin were EGFP-positive (Fig. 2A). Moreover, when dissociated and passaged at low density, cells in these spheres self-renewed and generated new EGFP-positive spheres. In contrast, almost all primary spheres from dorsal skin were EGFP-negative (Fig. 2B), and, after passaging, virtually none of the secondary SKP spheres expressed EGFP, indicating that only the EGFP-negative cells could self-renew.

To ask whether Wnt1-cre-positive facial SKPs derive from both whisker and hair follicles, we cultured cells from *Wnt1-cre;Z/EG* whisker pad versus nonwhisker-pad frontal facial skin under SKPs conditions. Both tissues generated EGFP-positive SKP spheres (Fig. 2C, 2D) that could be passaged, and that expressed vimentin, PDGFR*α* (Fig. 2C, 2D), nestin, and fibronectin (data not shown), all markers typical of SKP spheres. Thus, neural crest-derived facial SKPs derive from hair as well as whisker follicles.

To confirm that facial but not dorsal SKPs derive from the neural crest, we used flow cytometry to sort EGFP-positive and EGFP-negative cells from *Wnt1-cre;Z/EG* facial and dorsal skin samples that contained both the epidermis and the dermis (Fig. 2E, 2F). Approximately 30% of facial and 2% of dorsal skin cells expressed robust levels of EGFP, consistent with the immunocytochemical results. When these sorted cells were cultured at low density, very different results were obtained for facial versus dorsal cells. In facial skin, almost all of the primary sphere-forming ability was present in the EGFP-positive cells, although the occasional sphere was generated from the EGFP-negative fraction, potentially because the reporter is not 100% penetrant. These EGFP-positive spheres could be passaged and would self-renew to generate EGFP-positive secondary spheres (Fig. 2G). For dorsal skin, virtually all of the sphere-forming ability was present within the EGFP-negative population, and these EGFP-negative spheres self-renewed. In contrast, only very few small primary spheres formed from the EGFP-positive population, and these spheres did not self-renew when passaged (Fig. 2H). Thus, SKPs derive from *Wnt1*-expressing neural crest in facial, but not dorsal dermis, consistent with the in vivo lineage tracing.

Dorsal Trunk SKPs and Their Hair Follicle Niche Are Somite-Derived

The dorsal trunk dermis arises from the somites [22, 36] suggesting that, despite their similarities to neural crest precursors, dorsal follicle dermal precursors, and the SKPs they generate might also derive from this embryonic origin. To address this possibility, we utilized a transgenic *Myf5-cre* mouse, where cre recombinase is expressed in cells deriving from the somites [26, 30], and crossed it to *R26R* reporter mice that carry a floxed *β-galactosidase* allele in the *ROSA26* locus [28]. In these mice, somite-derived cells will express *β*-galactosidase. X-gal staining of neonatal dorsal skin from these mice demonstrated that, as predicted by their somite origin, most dermal cells were *β*-galactosidase-positive (data not shown). Moreover, both X-gal staining and immunocytochemistry for *β*-galactosidase (Fig. 3A) demonstrated that hair follicle DP and DS cells expressed *β*-galactosidase, indicating that they too were somite-derived. In contrast, dermal cells of facial skin, including those associated with hair follicles, were *β*-galactosidase-negative (Fig. 3B), as predicted by their neural crest origin.

To more definitively identify the cell types that were somite-derived within the dorsal dermis, we crossed the *Myf5-cre* mice to the *R26YFP* mouse that has a floxed *EYFP* allele in the same *ROSA26* locus [27]. These mice express EYFP in cells of the somite lineage. Double-label immunocytochemistry for EYFP and the dermal fibroblast marker fibronectin on neonatal dorsal skin demonstrated that EYFP was expressed in fibronectin-positive cells of interfollicular and follicular dermis (Fig. 3C). A similar analysis for EYFP and NCAM, a DP and DS marker that is expressed in the endogenous *sox2*-positive dermal precursors [7], demonstrated that the follicle dermal precursors also express EYFP (Fig. 3D). In contrast,

EYFP was not expressed in NCAM-positive follicle DP and DS cells in facial skin (Fig. 3E), although it was expressed in muscle cells (Fig. 3E). Analysis of EYFP in ventral dermis showed that interfollicular dermal cells as well as follicle DP and DS cells were negative for EYFP (Fig. 3F), consistent with a lateral plate rather than somite origin for this region of the trunk dermis.

These findings predict that dorsal but not ventral trunk SKPs are somite-derived. To test this prediction, we cultured cells from dorsal skin of neonatal *Myf5-cre;R26R* mice under SKP conditions at low density. For comparison, we cultured facial and ventral skin from the same mice. These cells were then passaged once at clonal density [6]. X-gal staining of the resultant secondary spheres demonstrated that virtually all SKP spheres isolated from dorsal back but not ventral trunk or facial skin expressed *β*-galactosidase (Fig. 3G). Thus, follicle dermal precursors and the SKPs they generate derive from a number of distinct developmental origins, as does the dermis itself.

Neural Crest- and Somite-Derived SKPs Are Similar and Both Populations Generate Functional Schwann Cells

Our previous work showed that both dorsal and facial SKPs self-renew, and that both can differentiate into *β*III-tubulin-positive neurons and smooth muscle actin (SMA)-positive myofibroblasts [6, 7]. Moreover, we have previously shown that dorsal SKPs generate bona fide Schwann cells [3, 5], a cell type thought to be only neural crest-derived. These findings suggest that, despite their differing developmental origins, these two populations of neural crest-like stem cells are functionally similar. To address this idea more definitively, we performed a series of side-by-side comparisons. Initially, we characterized the two populations with regard to a series of SKP markers, fibronectin, vimentin, nestin, and versican; immunostaining demonstrated that both populations expressed these markers (Fig. 4A). We then quantitatively characterized their proliferation and self-renewal. For proliferation, SKPs were grown under standard conditions in FGF2 and EGF and were passaged once at similar densities, and 8 days later, these secondary spheres were analyzed by immunostaining for Ki67, a proliferation marker. Approximately 4% of the cells in both facial and back skin SKP spheres were actively proliferating at this timepoint (Fig. 4B, 4C). To assess self-renewal, primary SKP spheres from facial and dorsal skin were dissociated to single cells that were then cultured at clonal density in methylcellulose-containing medium, and the number of new spheres were quantified [6]. This analysis demonstrated that both populations generated approximately 1%–2% secondary spheres (Fig. 4D). Together with our previous data, these findings indicate that SKPs from both facial and dorsal skin are similar, at least with regard to their proliferation, self-renewal, and differentiation ability.

One surprising inference of this work is that somite-derived dermal precursors can apparently generate Schwann cells. To more definitively test this idea, we first confirmed that total dorsal SKPs could generate Schwann cells, as we published previously [3] by differentiating them under previously defined conditions [4]. Immunocytochemistry revealed that dorsal SKPs generated bipolar cells that expressed the Schwann cell markers, S100*β* and GFAP (Fig. 5A), as did facial SKPs (Fig. 5A). To ask whether these two SKP populations were equally efficient at generating these Schwann-like cells, we generated neonatal facial and dorsal SKPs at low density, passaged them once, and then differentiated single, isolated SKP spheres under Schwann cell conditions, as we have described previously [3]. Immunostaining 2 weeks later for S100*β* and GFAP demonstrated that 48% and 44% of facial versus dorsal SKP spheres generated bipolar, Schwann-like cells.

These data indicate that dorsal SKPs are similar to facial SKPs in their ability to generate cells with Schwann cell characteristics. To definitively establish that somite-derived precursors could generate functional Schwann cells, we sorted EYFP-positive and EYFP-

negative cells from the dorsal skin of neonatal Myf5-cre;R26YFP mice (Fig. 5B). We then grew the EYFP-positive and EYFP-negative skin cells under SKP conditions. As predicted, the vast majority of SKP spheres were generated from the EYFP-positive cells, and all of these spheres were EYFP-positive (Fig. 5C). We then differentiated these EYFP-positive, somite-derived SKPs under Schwann cell conditions [4]. After 3 weeks, cultures were largely composed of two EYFP-positive cell populations, that is, flat cells with large nuclei and smaller bipolar cells with a Schwann cell morphology (Fig. 5D). Immunocytochemistry revealed that these EYFP-positive spindle-shaped cells expressed the Schwann cell markers P0, p75NTR and S100*β*, whereas the flat cells were negative for these markers (Fig. 5D).

We then asked whether these putative Schwann cells were functional by coculturing them with axons of sympathetic neurons that were grown in compartmented cultures. In these cultures, neuronal cell bodies are plated in central compartments, and then grow their axons into sealed side compartments [33]. EYFP-positive cells were sorted from dorsal skin of neonatal *Myf5-cre;R26YFP* mice, were grown as primary SKP spheres, and then differentiated under Schwann cell conditions for 3–4 weeks. These differentiated cultures, which contained a subpopulation of cells with an appropriate Schwann cell morphology, were then plated in side compartments that contained axons but not neuronal cell bodies. Immunostaining 8 days later showed that many EYFP-positive cells had associated with *β*III-tubulin-positive axons and that these expressed the peripheral myelin protein P0 (Fig. 5E). These results were indistinguishable from those obtained when cultured, peripheral nerve-derived Schwann cells were plated in similar cultures (data not shown). These data together with our previous findings that SKPs generated from dorsal trunk skin associate with an myelinate axons when transplanted into the peripheral nerve [3] provide strong evidence that somite-derived SKPs generate functional Schwann cells, a cell previously thought to only be generated by neural crest precursors.

SKPs of Distinct Developmental Origins are Highly Similar at the Transcriptional Level and Differ from Bone Marrow MSCs

To more comprehensively define how similar these developmentally distinct populations of SKPs are, we performed global gene expression analysis of adult SKPs derived from skin of dorsal trunk, ventral trunk, and the face. For comparison, we analyzed another adult stem cell with mesenchymal potential, bone marrow-derived MSCs. To perform this analysis, we compared three independent isolates each of dorsal trunk SKPs, ventral trunk SKPs, and facial SKPs and four isolates of MSCs, all generated from adult rats. RNA samples deriving from these cells were then analyzed on the Affymetrix GeneChip Rat Gene 1.0 ST Array. Spearman rank correlations, computed between each sample pair based on the microarray expression profiles demonstrated that dorsal, ventral, and facial SKPs were virtually identical (Fig. 6A). In contrast to this high similarity between dorsal, ventral, and facial SKPs, all three populations were different from adult MSCs (Fig. 6A). Cluster analysis, performed on the samples using a standard hierarchical clustering algorithm (correlation distance, average linkage clustering), confirmed these conclusions, demonstrating that the three SKPs populations grouped together, and that all three were distinct from the MSC samples (Fig. 6B).

To delineate the extent of differences between the transcriptomes of the neural crest-derived facial SKPs and somite-derived SKPs versus MSCs, we performed three-way differential expression analysis, similar to a one-way ANOVA, using the LIMMA bioconductor package [34, 37]. The Venn diagrams show the numbers of significantly differentially expressed genes ($p < .05$, BH) that are in common among the comparisons (Fig. 6C). Taken together, a total of 2,603 genes showed evidence of differential expression among any of the three groups; the expression levels of these genes are provided as a heatmap (Fig. 6D). Of these genes, only 106 were significantly different between dorsal and facial SKPs, while 2,233

and 2,525 differed between MSCs versus dorsal SKPs and MSCs versus facial SKPs, respectively.

These data argue that precursor cells of at least two, and potentially three, different developmental origins converge on to a highly similar phenotype. We therefore directly compared the expression of genes associated with neural crest specification [38], focusing on *Slug*, *Snail*, *Twist*, *Sox9*, *Sox10*, *Foxd3*, and *Ap2a1*. Heatmaps of the microarray data showed that these genes were expressed at similar levels in all three of the adult rat SKP samples, as were *p75NTR* and *RhoB*, which are also associated with neural crest precursors (Fig. 7A) [39, 40]. Reverse transcription polymerase chain reaction (RT-PCR) analyses of neonatal murine skin confirmed that these mRNAs were also expressed at similar levels in neonatal murine dorsal versus facial SKPs (Fig. 7B).

Developmentally Distinct Sox2-EGFP-Positive Dermal Precursors and the SKPs They Generate Maintain a Lineage History at the Gene Expression Level

Although these analyses indicate that mesenchymal precursors of different developmental origins converge to a very similar adult precursor phenotype, a standard pairwise differential expression comparison of facial versus dorsal trunk SKPs and dorsal trunk versus ventral trunk SKPs using linear models demonstrated that a subset of genes were significantly differentially expressed ($p < .05$, BH; Fig. 7C, 7D; Supporting Information Tables 1 and 2). Of the 35 most differentially expressed genes in the facial versus dorsal comparison, 10 were higher in dorsal SKPs and 25 in facial SKPs. Of the 35 most differentially expressed genes in the dorsal versus ventral comparison, four were higher in dorsal SKPs and 31 in ventral SKPs (Supporting Information Tables 1 and 2). Intriguingly, many of these genes are important during embryogenesis. In particular, dorsal trunk SKPs express high levels of the *Zic1* transcription factor relative to both facial and ventral trunk SKPs and the hox transcription factors *Hoxa5*, *Hoxc4*, *Hoxc6*, and *Hoxc9* relative to facial SKPs (Fig. 7D; Supporting Information Table 1). In contrast, facial SKPs expressed high relative levels of *Pax3*, and *Msx1*, both of which are transcription factors associated with cranial neural crest cells [41, 42], and *Mab-21-like 1* and *2*, mammalian homologues of the C. elegans *mab-21* cell fate gene that are expressed during embryogenesis [43] (Fig. 7D; Supporting Information Table 1). The relative enrichment of these different mRNAs was confirmed by RT-PCR analysis of neonatal murine dorsal versus facial SKPs (Fig. 7E).

To ask whether these differences were also seen in the endogenous dermal precursors that give rise to SKPs, we used flow cytometry to prospectively isolate EGFP-positive cells from facial versus dorsal skin of *Sox2-EGFP* neonatal mice. In these mice, EGFP is knocked-in to the *Sox2* locus [31], and this *Sox2-EGFP* reporter is selectively expressed in follicle DP and DS cells [7, 44]. We then performed RT-PCR analysis on these two cell populations. This analysis demonstrated that *Mab21-like-1* and *2*, *Eya1*, and *Pax3* mRNAs were all enriched in facial EGFP-positive precursors (Fig. 7F) as they were in facial SKPs. In contrast, *Zic1*, *Hoxa5*, *Hoxc6*, *Hoxc4*, and *Hoxc9* mRNAs were all highly enriched in dorsal EGFP-positive precursors, as they were in dorsal SKPs (Fig. 7F). Thus, although these different dermal precursor populations are highly similar, they maintain a history of their distinct developmental origins.

Discussion

The data presented here support three conclusions. First, they indicate that SKPs and the dermal precursors from which they arise are generated by multiple developmental lineages. Specifically, the lineage tracing indicates that follicle DS and DP cells derive from the neural crest in the face and from the somites in the dorsal trunk, as do SKPs themselves. Although we have not definitively established the origin of ventral trunk SKPs, we show

that they do not arise from the somites, and it is likely that, like the dermis, they derive from the lateral plate. Second, our findings demonstrate that, despite their different developmental origins, facial and dorsal SKPs are functionally similar and, perhaps most surprisingly, that somite-derived SKPs can generate a functional neural crest cell type, Schwann cells. Finally, the microarray analysis emphasizes the similarities between facial, dorsal trunk, and ventral trunk SKPs, showing that they are highly similar to each other at the transcriptional level but different from another adult mesenchymal precursor, bone-marrow derived MSCs. Intriguingly, these gene expression studies also defined a number of embryonic transcription factors that are highly differentially expressed in facial versus dorsal trunk SKPs, and in the Sox2-positive dermal precursors from which they derive. Thus, despite their similarities, these dermal precursors maintain a memory of their developmental origins. These findings demonstrate that dermal stem cells are generated by distinct convergent developmental pathways, and indicate that adult stem cells with almost indistinguishable phenotypes can be generated from multiple developmental lineages.

Previous work showed that SKPs display similarities to neural crest precursors; they express neural crest markers, differentiate into neural and mesodermal lineages, and migrate like embryonic neural crest precursors when transplanted into the embryonic chick neural crest migratory stream [6]. We also showed previously that SKPs differentiated into functional Schwann cells, a cell type that is only thought to be generated from neural crest [3, 5]. Importantly, data presented here indicate that dorsal SKPs that are definitively marked as being of a somite origin also generate Schwann cells, a surprising finding. Do the endogenous *Sox2*-positive precursors that generate SKPs ever differentiate into Schwann cells in vivo? Previous work indicates that follicle dermal precursors differentiate into dermal cell types and induce hair follicle morphogenesis, but there are no data to indicate that they generate other neural crest derivatives in vivo. However, when these *Sox2*-positive precursors are directly differentiated in culture, without going through a SKPs intermediate, they do in fact generate cells with characteristics of *β*III-tubulin-positive neurons [7], and microarray analysis indicates that they express many markers similar to neural crest precursors [7]. Similar results have been obtained for DP cells isolated using other approaches [6, 44–46], confirming these findings. We therefore propose that, as seen with embryonic neural crest precursors [9], follicle dermal precursors have a broader differentiation potential than they usually display in vivo, and that their dermal environment restricts their differentiation to appropriate cell types. A key question for the future will be whether or not this broader potential is ever unmasked in vivo either under basal conditions and/or following injury.

Our finding that hair follicle DP and DS from dorsal trunk skin derive from a nonneural crest origin does not rule out the possibility that other neural crest-derived precursors reside in hair follicles. In particular, previous work defined a population of neural crest precursors within the follicle bulge region that, like SKPs, can generate peripheral neural progeny and some mesenchymal derivatives [17] and lineage tracing demonstrated *Wnt-1cre;R26R*-positive cells located in close proximity to the bulge region [35]. Here, we have confirmed the presence of *Wnt1-cre;Z/EG*-positive cells in p75NTR-positive nerves that were very closely associated with the bulge region. This finding is particularly intriguing in light of a recent report showing that multipotent neural crest precursors enter the skin via peripheral nerves and contribute melanocytes during embryogenesis [11]. Although our sorting data argue that these *Wnt-1-cre;Z/EG*-positive cells do not generate SKPs, it is nonetheless possible that they play a key role in vivo either by contributing melanoblasts to the follicle and/or Schwann cells to nerve endings.

The experiments presented here have used a number of different *Cre* reporter lines to perform lineage tracing, and the data must therefore be interpreted in light of the limitations

of this approach. We previously utilized *β*-galactosidase expression in a *Wnt1-cre;R26R* mouse to establish that facial SKPs and the follicle DP and DS niche from which they originate are neural crest-derived. In that same study, we reported a small number of *β*-galactosidase-positive cells within and/or adjacent to dorsal trunk follicle DP and interpreted those findings as indicative of a neural crest origin for at least some of these DP cells. Here, our double-label immunocytochemical analysis of dorsal trunk skin sections from *Wnt1-cre;Z/EG* mice showed that tyrosinase-positive melanocytes, but not NCAM-positive DP cells, expressed EGFP. These findings, combined with our data showing that dorsal skin DP were genetically tagged in *Myf5-cre:R26R* and *Myf5-cre;R26YFP* mice strongly argue that dorsal trunk DP and DS cells are somite-derived.

The concept that cells of two developmental origins can converge on to a similar cellular phenotype is not a new one, particularly with regard to neural crest derivatives. For example, all of the mesenchymal derivatives of the face, including bone, cartilage, and dermis, derive from the neural crest [9, 21], whereas those of the body derive from the somites or the lateral plate [22, 23]. Thus, neural crest cells can and do generate mesodermal progeny. Although there is no direct precedent for mesodermal precursors generating neural crest-specific progeny such as cells of the peripheral nervous system, it is intriguing that many nonneural crest-derived tissues contain neuroendocrine cell types similar to those generated from the neural crest. Our finding that cells of nonneural crest origin can converge on to a phenotype with similarities to neural crest precursors suggests that perhaps a neural crest-like precursor may play an important role in these tissues. A good example of this would be the pancreas which for many years was thought to be at least in part neural crest-derived because of the endocrine and exocrine cells that it contains.

Our large-scale gene expression analyses indicate that, despite their different developmental origins, facial, dorsal trunk, and ventral trunk SKPs are highly similar. However, all of these populations are distinct from another adult mesenchymal precursor, bone marrow-derived MSCs. These results are in good agreement with the functional properties of these different populations. Dorsal and facial SKPs are almost indistinguishable with regard to their growth and differentiation in culture, and transplant studies indicate that they are apparently interchangeable with regard to transplantation into facial or dorsal trunk skin environments (J.A.B., H.J., F.D.M., unpublished data). In contrast, although both SKPs and MSCs can generate cells such as adipocytes, cartilage, and bone cells in culture [2, 47], when transplanted into the dermis MSCs neither home to a DP niche, as do SKPs, nor do they induce hair follicle morphogenesis [7]. Thus, SKPs and MSCs are two different precursor populations, despite a partially shared differentiation potential. Intriguingly, during embryogenesis, neural crest stem cells give rise to bone marrow MSCs [48], suggesting a parent-progeny relationship between these different precursors and raising the possibility that neural crest-like precursors, perhaps of nonneural crest origin, continue to give rise to MSCs in adulthood.

Together, these data support the concept that a stem cell of non-neural crest origin can generate peripheral neural cells that are only thought to derive from the neural crest. These findings raise some interesting questions with regard to the gene-directed transdifferentiation of dermal fibroblasts into neurons [49]. Although in studies of this type, it is assumed that dermal fibroblasts represent a homogeneous population that are committed to a fibroblast lineage, findings presented here indicate that a subset of dermal cells are endogenous multipotent precursors and that the genesis of neurons from these precursors may reflect the unmasking of the endogenous potential of these cells rather than transdifferentiation. Whether similar multipotent cells reside within other tissues and/or whether they also have the potential to generate peripheral neural or neuroendocrine cell types is a key question for the future.

Supplementary Material

Refer to Web version on PubMed Central for supplementary material.

Acknowledgments

We thank Shaalee Dworski, Asli Dedeagac, Vanessa Seale, Smitha Paul, and Dennis Aquino for experimental help, and David Kaplan for advice. This work was supported by grants from the Canadian Institutes of Health Research and the HHMI. F.D.M. is a HHMI International Research Scholar and a Canada Research Chair and M.A.M a Michael Smith Foundation Senior Scholar. H.J. was supported by a studentship from HSC Research Institute and O.M. by studentships from NSERC and the Michael Smith Foundation.

References

1. Toma JG, Akhavan M, Fernandes KJ, et al. Isolation of multipotent adult stem cells from the dermis of mammalian skin. Nat Cell Biol. 2001; 3:778–784. [PubMed: 11533656]
2. Lavoie JF, Biernaskie JA, Chen Y, et al. Skin-derived precursors differentiate into skeletogenic cell types and contribute to bone repair. Stem Cells Dev. 2009; 18:893–906. [PubMed: 18834279]
3. McKenzie IA, Biernaskie J, Toma JG, et al. Skin-derived precursors generate myelinating Schwann cells for the injured and dysmyelinated nervous system. J Neurosci. 2006; 26:6651–6660. [PubMed: 16775154]
4. Biernaskie JA, McKenzie IA, Toma JG, et al. Isolation of skin-derived precursors (SKPs) and differentiation and enrichment of their Schwann cell progeny. Nat Protoc. 2006; 1:2803–2812. [PubMed: 17406538]
5. Biernaskie J, Sparling JS, Liu J, et al. Skin-derived precursors generate myelinating Schwann cells that promote remyelination and functional recovery after contusion spinal cord injury. J Neurosci. 2007; 27:9545–9559. [PubMed: 17804616]
6. Fernandes KJ, McKenzie IA, Mill P, et al. A dermal niche for multipotent adult skin-derived precursor cells. Nat Cell Biol. 2004; 6:1082–1093. [PubMed: 15517002]
7. Biernaskie J, Paris M, Morozova O, et al. SKPs derive from hair follicle precursors and exhibit properties of adult dermal stem cells. Cell Stem Cell. 2009; 5:610–623. [PubMed: 19951689]
8. Su X, Paris M, Gi YJ, et al. TAp63 prevents premature aging by promoting adult stem cell maintenance. Cell Stem Cell. 2009; 5:64–75. [PubMed: 19570515]
9. Le Douarin, N. The Neural Crest. Cambridge: Cambridge University Press; 1982. p. xip. 259
10. Jessen KR, Mirsky R. The origin and development of glial cells in peripheral nerves. Nat Rev. 2005; 6:671–682.
11. Adameyko I, Lallemend F, Aquino JB, et al. Schwann cell precursors from nerve innervation are a cellular origin of melanocytes in skin. Cell. 2009; 139:366–379. [PubMed: 19837037]
12. Li HY, Say EH, Zhou XF. Isolation and characterization of neural crest progenitors from adult dorsal root ganglia. Stem Cells. 2007; 25:2053–2065. [PubMed: 17525237]
13. Nagoshi N, Shibata S, Kubota Y, et al. Ontogeny and multipotency of neural crest-derived stem cells in mouse bone marrow, dorsal root ganglia, and whisker pad. Cell Stem Cell. 2008; 2:392–403. [PubMed: 18397758]
14. Kruger GM, Mosher JT, Bixby S, et al. Neural crest stem cells persist in the adult gut but undergo changes in self-renewal, neuronal subtype potential, and factor responsiveness. Neuron. 2002; 35:657–669. [PubMed: 12194866]
15. Tomita Y, Matsumura K, Wakamatsu Y, et al. Cardiac neural crest cells contribute to the dormant multipotent stem cell in the mammalian heart. J Cell Biol. 2005; 170:1135–1146. [PubMed: 16186259]
16. Wong CE, Paratore C, Dours-Zimmermann MT, et al. Neural crest-derived cells with stem cell features can be traced back to multiple lineages in the adult skin. J Cell Biol. 2006; 175:1005–1015. [PubMed: 17158956]
17. Sieber-Blum M, Grim M, Hu YF, et al. Pluripotent neural crest stem cells in the adult hair follicle. Dev Dyn. 2004; 231:258–269. [PubMed: 15366003]

18. Yoshida S, Shimmura S, Nagoshi N, et al. Isolation of multipotent neural crest-derived stem cells from the adult mouse cornea. Stem Cells. 2006; 24:2714–2722. [PubMed: 16888282]
19. Pardal R, Ortega-Saenz P, Duran R, et al. Glia-like stem cells sustain physiologic neurogenesis in the adult mammalian carotid body. Cell. 2007; 131:364–377. [PubMed: 17956736]
20. Widera D, Zander C, Heidbreder M, et al. Adult palatum as a novel source of neural crest-related stem cells. Stem Cells. 2009; 27:1899–1910. [PubMed: 19544446]
21. Couly G, Grapin-Botton A, Coltey P, et al. Determination of the identity of the derivatives of the cephalic neural crest: incompatibility between Hox gene expression and lower jaw development. Development. 1998; 125:3445–3459. [PubMed: 9693148]
22. Mauger A. The role of somitic mesoderm in the development of dorsal plumage in chick embryos. II. Regionalization of the plumage-forming mesoderm. J Embryol Exp Morphol. 1972; 28:343–366. [PubMed: 4642992]
23. Christ B, Ordahl CP. Early stages of chick somite development. Anat Embryol. 1995; 191:381–396. [PubMed: 7625610]
24. Danielian PS, Muccino D, Rowitch DH, et al. Modification of gene activity in mouse embryos in utero by a tamoxifen-inducible form of Cre recombinase. Curr Biol. 1998; 8:1323–1326. [PubMed: 9843687]
25. Novak A, Guo C, Yang W, et al. Z/EG, a double reporter mouse line that expresses enhanced green fluorescent protein upon Cre-mediated excision. Genesis. 2000; 28:147–155. [PubMed: 11105057]
26. Tallquist MD, Weismann KE, Hellstrom M, et al. Early myotome specification regulates PDGFA expression and axial skeleton development. Development. 2000; 127:5059–5070. [PubMed: 11060232]
27. Srinivas S, Watanabe T, Lin CS, et al. Cre reporter strains produced by targeted insertion of EYFP and ECFP into the ROSA26 locus. BMC Dev Biol. 2001; 1:4. [PubMed: 11299042]
28. Soriano P. Generalized lacZ expression with the ROSA26 Cre reporter strain. Nat Genet. 1999; 21:70–71. [PubMed: 9916792]
29. Kuang S, Kuroda K, Le Grand F, et al. Asymmetric self-renewal and commitment of satellite stem cells in muscle. Cell. 2007; 129:999–1010. [PubMed: 17540178]
30. Hosokawa R, Urata M, Han J, et al. TGF-beta mediated Msx2 expression controls occipital somites-derived caudal region of skull development. Dev Biol. 2007; 310:140–153. [PubMed: 17727833]
31. Ellis P, Fagan BM, Magness ST, et al. SOX2, a persistent marker for multipotential neural stem cells derived from embryonic stem cells, the embryo or the adult. Dev Neurosci. 2004; 26:148–165. [PubMed: 15711057]
32. Yang Y, Rossi FM, Putnins EE. Ex vivo expansion of rat bone marrow mesenchymal stromal cells on microcarrier beads in spin culture. Biomaterials. 2007; 28:3110–3120. [PubMed: 17433434]
33. Singh KK, Miller FD. Activity regulates positive and negative neurotrophin-derived signals to determine axon competition. Neuron. 2005; 45:837–845. [PubMed: 15797546]
34. Smyth GK. Linear models and empirical bayes methods for assessing differential expression in microarray experiments. Stat Appl Genet Mol Biol. 2004; 3:Article3. [PubMed: 16646809]
35. Sieber-Blum M, Grim M. The adult hair follicle: Cradle for pluripotent neural crest stem cells. Birth Defects Res C Embryo Today. 2004; 72:162–172. [PubMed: 15269890]
36. Olivera-Martinez I, Thelu J, Dhouailly D. Molecular mechanisms controlling dorsal dermis generation from the somitic dermomyotome. Int J Dev Biol. 2004; 48:93–101. [PubMed: 15272374]
37. Wettenhall JM, Smyth GK. limmaGUI: A graphical user interface for linear modeling of microarray data. Bioinformatics (Oxford, England). 2004; 20:3705–3706.
38. Sauka-Spengler T, Meulemans D, Jones M, et al. Ancient evolutionary origin of the neural crest gene regulatory network. Dev Cell. 2007; 13:405–420. [PubMed: 17765683]
39. Stemple DL, Anderson DJ. Isolation of a stem cell for neurons and glia from the mammalian neural crest. Cell. 1992; 71:973–985. [PubMed: 1458542]
40. Liu JP, Jessell TM. A role for rhoB in the delamination of neural crest cells from the dorsal neural tube. Development. 1998; 125:5055–5067. [PubMed: 9811589]

41. Tremblay P, Kessel M, Gruss P. A transgenic neuroanatomical marker identifies cranial neural crest deficiencies associated with the Pax3 mutant Splotch. Development. 1995; 171:317–329.

42. Han J, Ishii M, Bringas P Jr, et al. Concerted action of Msx1 and Msx2 in regulating cranial neural crest cell differentiation during frontal bone development. Mech Dev. 2007; 124:729–745. [PubMed: 17693062]

43. Wong YM, Chow KL. Expression of zebrafish mab21 genes marks the differentiating eye, midbrain and neural tube. Mech Dev. 2002; 113:149–152. [PubMed: 11960703]

44. Driskell RR, Giangreco A, Jensen KB, et al. Sox2-positive dermal papilla cells specify hair follicle type in mammalian epidermis. Development. 2009; 136:2815–2823. [PubMed: 19605494]

45. Rendl M, Lewis L, Fuchs E. Molecular dissection of mesenchymal-epithelial interactions in the hair follicle. Plos Biol. 2005; 3:e331. [PubMed: 16162033]

46. Hunt DP, Morris PN, Sterling J, et al. A highly enriched niche of precursor cells with neuronal and glial potential within the hair follicle dermal papilla of adult skin. Stem Cells. 2008; 26:163–172. [PubMed: 17901404]

47. Prockop DJ. Marrow stromal cells as stem cells for nonhematopoietic tissues. Science. 1997; 276:71–74. [PubMed: 9082988]

48. Takashima Y, Era T, Nakao K, et al. Neuroepithelial cells supply an initial transient wave of MSC differentiation. Cell. 2007; 129:1377–1388. [PubMed: 17604725]

49. Vierbuchen T, Ostermeier A, Pang ZP, et al. Direct conversion of fibroblasts to functional neurons by defined factors. Nature. 2010; 463:1035–1041. [PubMed: 20107439]

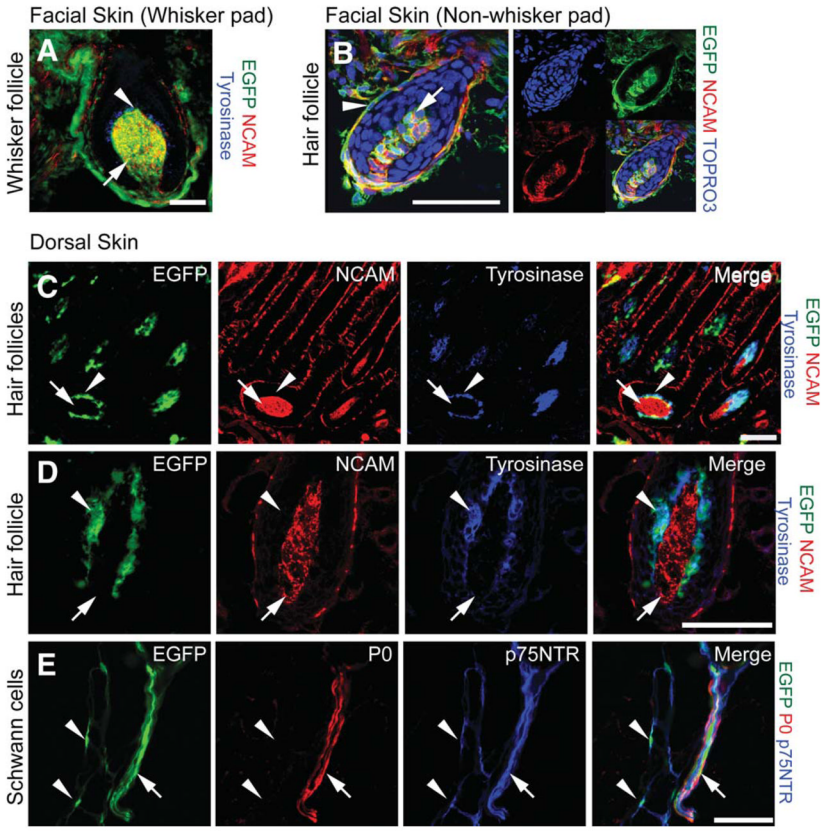

Figure 1.

In facial but not dorsal trunk skin, follicle dermal papilla (DP) and DS derive from the neural crest. (**A, B**): Immunocytochemistry of facial skin sections from neonatal *Wnt1-cre;Z/EG* mice. (**A**): Whisker follicle section immunostained for EGFP (green), the DP marker NCAM (red), and the melanoblast/melanocyte marker tyrosinase (blue). The arrow denotes the whisker follicle DP, and the arrowhead the overlying melanocytes. (**B**): A section through a hair follicle in facial skin outside of the whisker pad immunostained for EGFP (green) and the DP marker NCAM (red). Nuclei were stained with the dye TOPRO3 (blue). The arrow denotes the hair follicle DP, and the arrowhead the dermal sheath. (**C, D**): Dorsal trunk skin sections from neonatal *Wnt1-cre;Z/EG* mice, immunostained for EGFP (green), the DP marker NCAM (red), and the melanoblast/melanocyte marker tyrosinase (blue). Arrows denote the DP of dorsal hair follicles and arrowheads the overlying melanocytes. (**E**): Dorsal skin from neonatal *Wnt1-cre:Z/EG* mice, immunostained for EGFP (green) and the Schwann cell markers P0 peripheral myelin protein (red) and p75NTR (blue). Arrows denote a nerve containing myelinating Schwann cells positive for all three markers, whereas arrowheads indicate EGFP-positive, p75NTR-positive nonmyelinating Schwann cells. Scale bar = 50 μm (for all panels). Abbreviations: EGFP, enhanced green fluorescent protein; NCAM, neural cell adhesion molecule.

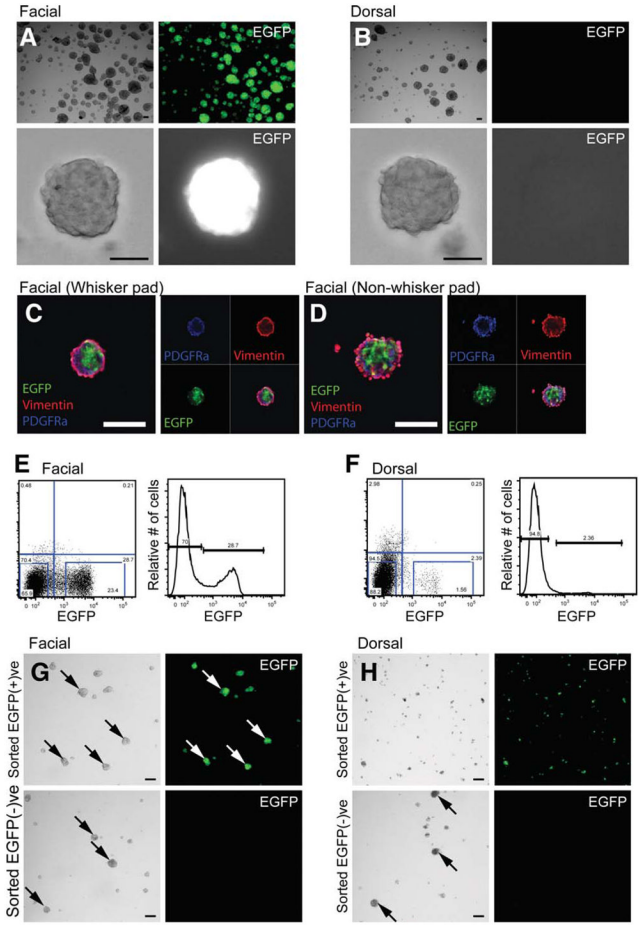

Figure 2.

In facial but not dorsal trunk skin, skin-derived precursors (SKPs) derive from neural crest. (**A, B**): Primary SKP spheres generated from neonatal *Wnt1-cre;Z/EG* facial (**A**) and dorsal trunk (**B**) skin. In the bottom panels, single spheres are shown at high magnification. Scale bar = 50 μm. (**C, D**): Primary facial SKP spheres from whisker pad skin and from facial skin outside of the whisker pad, immunostained for EGFP (green), and the SKP markers vimentin (red) and PDGFRα (blue). Scale bar = 100 μm. (**E, F**): Flow cytometry plots of neonatal *Wnt1-cre;Z/EG* facial (**E**) and dorsal trunk (**F**) skin, sorted on the basis of EGFP expression. Left panels show the primary data, with the bottom blue boxes indicating the cells that were collected for culture. Numbers represent the percentage of cells in each quadrant of the plot. Right panels show the data plotted as relative numbers of cells expressing no or high relative levels of EGFP. The percentage of cells in each of those two groups is indicated. (**G, H**): Skin cells sorted as in (**E, F**) were cultured in SKPs medium for 1–2 weeks, passaged, and photographed 1 week later. Arrows indicate secondary SKP spheres. For facial skin (**G**), the EGFP-positive cell fraction contained most of the SKP-forming activity, although some SKP spheres were generated from the EGFP-negative population. For dorsal trunk skin (**H**), EGFP-positive cells did not generate SKP spheres when passaged, but remained as single cells or small clumps of cells, and virtually all of the SKP-forming activity was present within the EGFP-negative cell fraction. Scale bar = 100 μm. Abbreviations: EGFP, enhanced green fluorescent protein; PDGFRα, platelet derived growth factor receptor α.

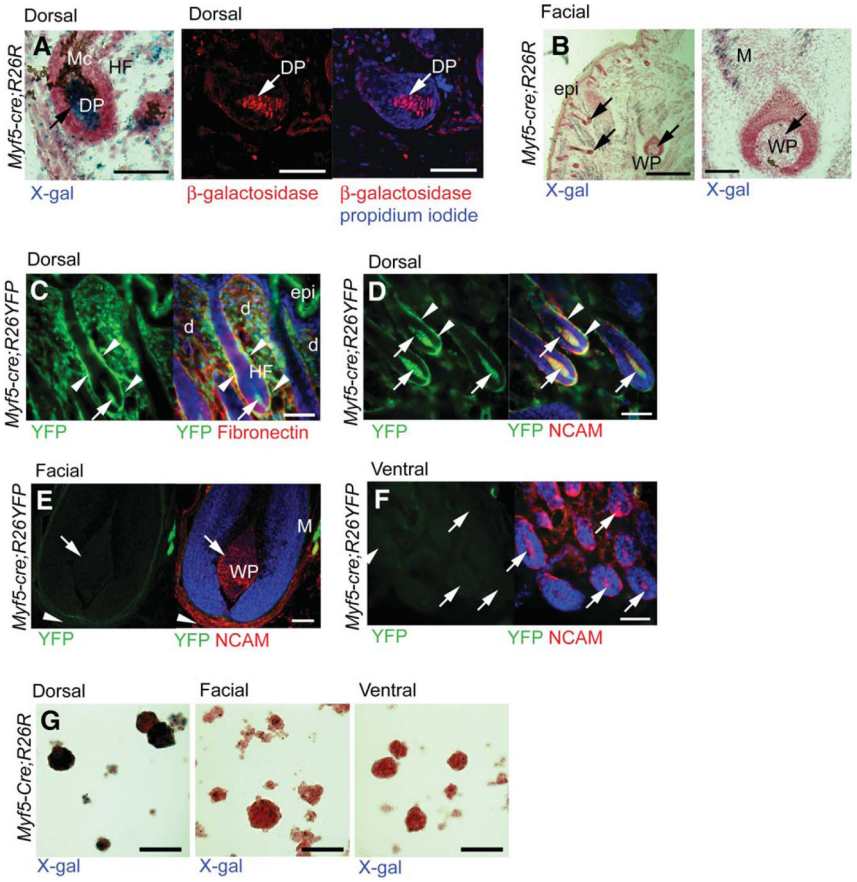

Figure 3.

In dorsal trunk but not facial or ventral trunk skin, hair follicle DP/dermal sheath (DS) and Skin-derived precursors (SKPs) derive from the somites. (**A, B**): Dorsal trunk (**A**) and facial (**B**) skin sections from neonatal *Myf5-cre;R26R* mice, stained with X-gal ([**A**], left panel and [**B**], blue) or immunostained for *β*-galactosidase ([**A**], middle and right panels, red) to detect *β*-galactosidase. Tissue was counterstained with nuclear fast red (red in [**A**], left panel and [**B**]) or propidium iodide (blue in [**A**], right panel) to show morphology. Arrows denote hair and whisker follicle DP. Scale bar = 50 *μ*m (**A**), 500 *μ*m ([**B**], left) and 100 *μ*m ([**B**], right). (**C–F**): Dorsal trunk (**C, D**), facial (**E**), and ventral trunk (**F**) skin sections from neonatal *Myf5-cre;R26YFP* mice, immunostained for EYFP (green), fibronectin ([**C**], red) or NCAM ([**D–F**], red). Tissues were counterstained with the nuclear dye TOPRO3 (blue) to show morphology. Arrows denote follicle DP, which are EYFP-positive in dorsal trunk skin (**C, D**), but not in facial (**E**) or ventral trunk (**F**) skin. Arrowheads denote EYFP-positive DS cells in dorsal trunk skin (**C, D**). Note that muscle cells (**M**) in facial skin (**E**) are EYFP-positive. Scale bar = 50 *μ*m. (**G**): Secondary SKP spheres generated from neonatal *Myf5-cre;R26R* dorsal trunk skin (left panel), facial skin (middle panel), and ventral trunk skin (right panel), stained with X-gal to detect *β*-galactosidase (blue) and counterstained with nuclear fast red (red). Scale bar = 200 *μ*m. Abbreviations: d, interfollicular dermis; DP, dermal papilla; epi, epidermis; HF, hair follicle; M, muscle; Mc, melanocytes; NCAM, neural cell adhesion molecule; WP, whisker papilla; YFP, yellow fluorescent protein.

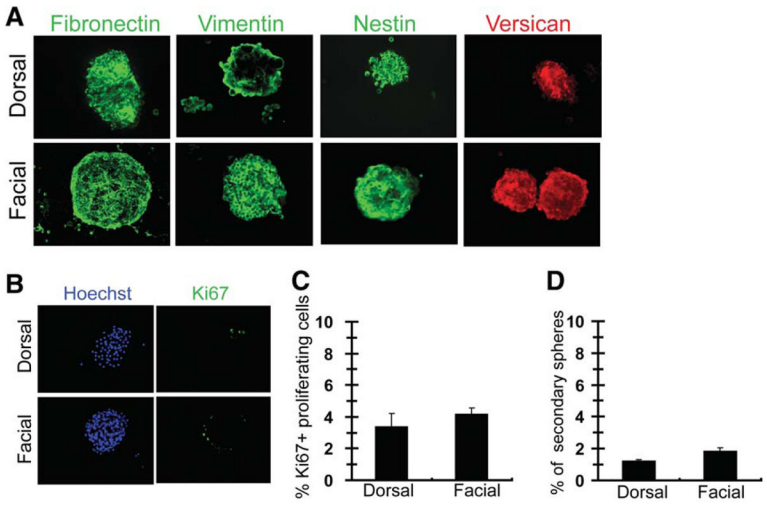

Figure 4.

Facial and dorsal trunk skin-derived precursors (SKPs) display similar properties. (**A**): Secondary SKP spheres generated from neonatal mouse dorsal trunk skin and facial skin, immunostained for fibronectin, vimentin, nestin, and versican. (**B**): Primary SKP spheres isolated from neonatal wild-type dorsal trunk skin and facial skin, immunostained for Ki67 (green), and counterstained with Hoechst to show cell nuclei (blue). (**C**): Quantification of Ki67-positive cells from experiments similar to that shown in (**B**). $n = 3$ independent experiments. (**D**): Quantification of the percentage of cells that form a new sphere from primary SKPs plated at clonal density (2,500 cells/ml) in methylcellulose cultures. $n = 3$ independent experiments.

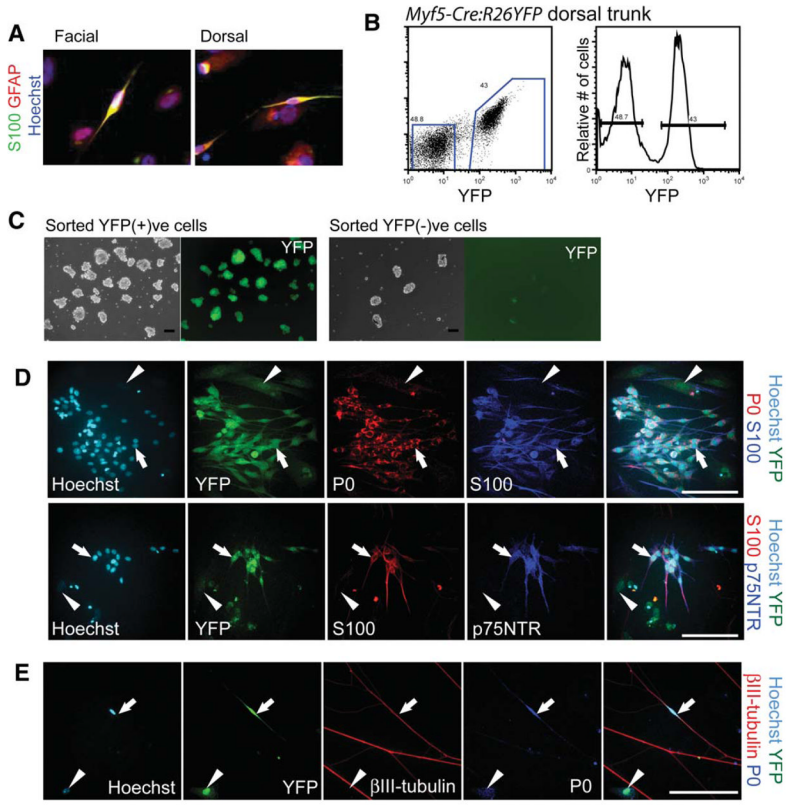

Figure 5.

Somite-derived skin-derived precursors (SKPs) generate Schwann cells. (**A**): Neonatal mouse dorsal trunk and facial skin cells cultured as SKPs, differentiated under gliogenic conditions for 2–3 weeks, and immunostained for the Schwann cell markers S100*β* (green) and GFAP (red), and counterstained with Hoechst (blue). (**B**): Flow cytometry plots of *Myf5-cre;R26YFP* dorsal trunk skin cells, sorted for relative levels of EYFP expression. The left panel shows the primary data, and the blue boxes show the cell fractions that were cultured as EYFP-positive versus negative cells. The right panel shows the same data plotted as relative cell numbers versus EYFP expression. The percentage of cells in each fraction is indicated. (**C**): Cells sorted as in (**B**) and cultured for 7 days in SKPs conditions. The left two panels show the SKP spheres derived from the EYFP-positive fraction and the right two panels show the EYFP-negative fraction, with the left panels of each pair showing phase illumination and the right the same fields with fluorescence illumination. (**D**): *Myf5-cre;R26YFP*-positive dorsal trunk SKPs were differentiated under gliogenic conditions for 2–3 weeks, and immunostained for EYFP (green), and the Schwann cell markers P0 (red, top panels) S100*β* (blue, top panels; red bottom panels) and p75NTR (blue, bottom panels). Arrows in top panels indicate EYFP-positive, P0-positive, S100*β*-positive spindle-shaped Schwann cells and in the bottom panels indicate EYFP-positive, S100*β*-positive, p75NTR-positive Schwann cells. Arrowheads indicate EYFP-positive, flat cells that are negative for the Schwann cell markers. Cells were counterstained with Hoechst (turquoise). Scale bar = 100 *μ*m. (**E**): Differentiated *Myf5-cre;R26YFP*-positive dorsal trunk SKPs were cocultured with axons of sympathetic neurons in compartmented cultures for 8 days, and immunostained for EYFP (green), the Schwann cell marker P0 (blue), and the axonal marker *β*III-tubulin (red). Arrows indicate a representative EYFP-positive, P0-positive, spindle-shaped Schwann cell associated with a *β*III-tubulin-positive axon. Arrowheads indicate an EYFP-positive, flat cell that is not associated with an axon and that is negative for Schwann

cell markers. Cells were counterstained with Hoechst (turquoise). Scale bar = 100 μm. Abbreviations: GFAP, glial fibrillary acidic protein; YFP, yellow fluorescent protein.

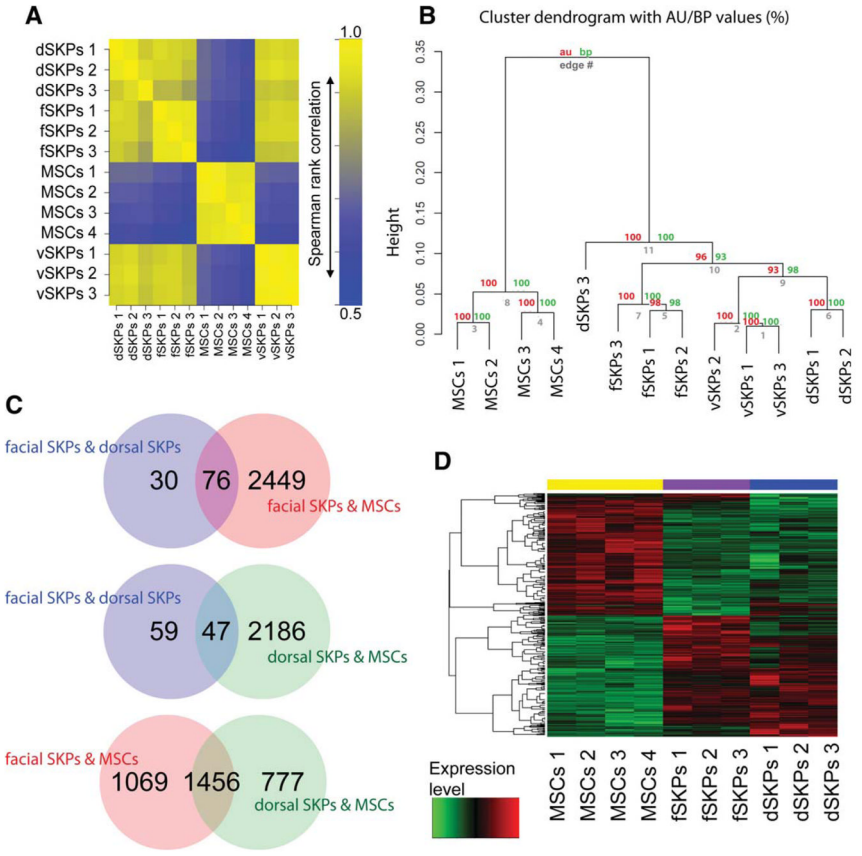

Figure 6.

Microarray analysis of adult dorsal trunk, ventral trunk, and facial SKPs versus MSCs. Microarray analysis was performed to compare gene expression patterns among adult rat dorsal trunk, facial, and ventral trunk SKPs. Adult rat bone marrow MSCs were used as a comparator. Three independent isolates of secondary passage SKPs from dorsal trunk skin (dSKPs 1–3), facial skin (fSKPs 1–3), ventral trunk skin (fSKPs 1–3), and four isolates of MSCs (MSCs 1–4) were compared. (**A**): Spearman rank correlation matrix computed for the microarray experiments based on the 3,182 probesets showing the most variation across the experiments, as visualized by color-coding, with yellow representing the most highly correlated samples, and blue the least correlated. Note that the dorsal trunk, facial, and ventral trunk SKP samples are highly correlated with each other, whereas they show less correlation with the MSCs. (**B**): Microarray datasets from all four sets of samples were clustered using hierarchical clustering with correlation distance and average linkage. The significance of the hierarchical clustering result was assessed using AU and BP resampling implemented in the R package pvclust. (**C**): Venn diagrams of pairwise comparisons between facial SKPs, dorsal trunk SKPs, and MSCs to identify genes differentially expressed between each pair of samples using an analysis similar to one-way ANOVA implemented in the LIMMA bioconductor package. The Venn diagrams show significantly differentially expressed genes ($p < .05$, Benjamini) that are in common among the pairwise comparisons, revealing that facial SKPs and dorsal SKPs are more similar to each other than either of them are to MSCs. (**D**): Three-way comparison was conducted across the groups to identify genes that show evidence of differential expression (analysis similar to one-way analysis of variance). Expression profiles of 2,603 genes, identified as differentially expressed ($p < .05$, Benjamini), are plotted as a heatmap. Abbreviations: AU, approximately

unbiased; BP, bootstrap probability; MSC, mesenchymal stromal cell; SKP, skin-derived precursor.

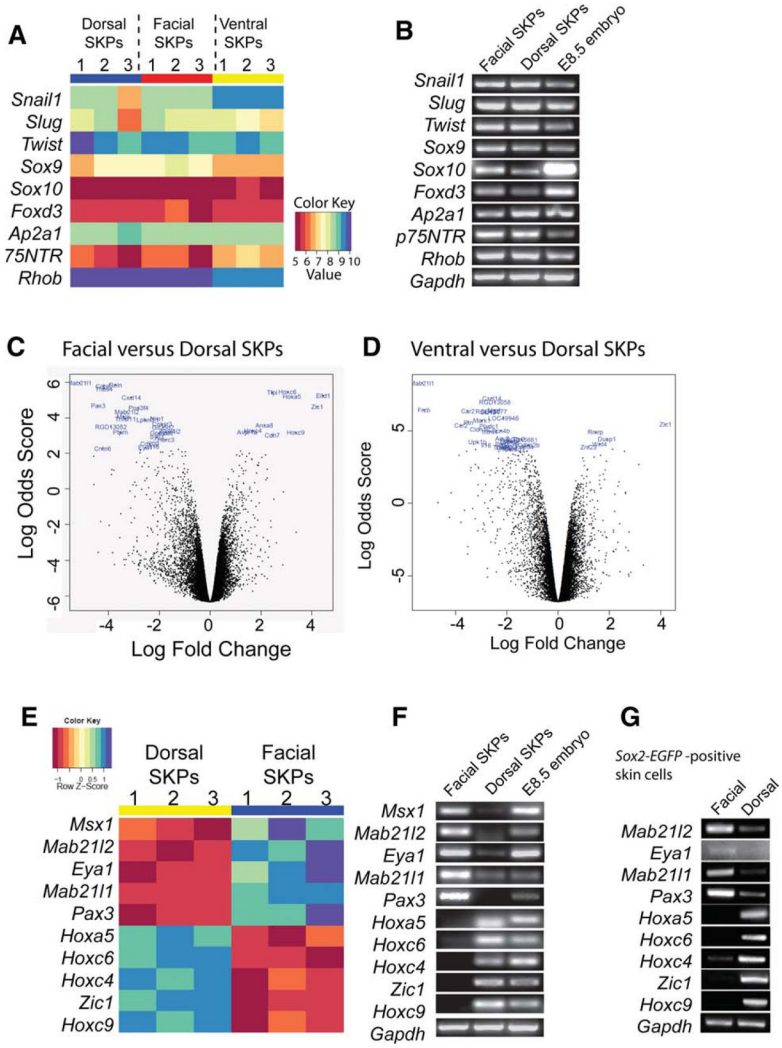

Figure 7.

SKPs of all developmental origins express neural crest signature genes but retain a lineage history at the gene expression level. (**A**): Microarray expression levels of genes expressed in embryonic neural crest precursors in adult rat facial, dorsal trunk, and ventral trunk SKPs, plotted as a heatmap. Red indicates the lowest relative levels of expression and dark blue the highest, as defined by the color key. (**B**): Reverse transcription polymerase chain reactions (RT-PCRs) for the same genes shown in (**A**), in total RNA isolated from neonatal murine dorsal trunk and facial secondary SKP spheres. Total RNA from E8.5 murine embryos was used as a positive control. (**C, D**): Pairwise differential expression analysis was conducted between (**C**) facial and dorsal trunk SKPs and (**D**) ventral trunk and dorsal trunk SKPs from adult rats using the LIMMA bioconductor package. The 35 genes showing most significant differential expression between the two populations on the volcano plots are shown and are listed in Supporting Information Tables 1 and 2, after multiple testing correction. The positive log fold changes indicate genes that are expressed at higher levels in dorsal SKPs (**C, D**), and the negative log fold changes those that are expressed at decreased levels in dorsal SKPs relative to facial SKPs (**C**) or ventral trunk SKPs (**D**). (**E**): Microarray expression levels of transcription factors that were identified as being among the most differentially expressed in the analysis in (**C**), plotted as a heatmap. (**F**): RT-PCRs for the genes highlighted in (**E**) in total RNA from neonatal murine dorsal and facial secondary

SKP spheres, highlighting the differential expression. Total RNA from E8.5 murine embryos was used as a positive control. (**G**): RT-PCRs for the genes highlighted in (**F**) in total RNA from uncultured, purified EGFP-positive cells from neonatal *Sox2-EGFP* mouse dorsal trunk and facial skin, highlighting differential expression in uncultured dermal precursors. Abbreviations: EGFP, enhanced green fluorescent protein; SKP, skin-derived precursor.